δ Scuti pulsations in the bright Pleiades eclipsing binary HD 23642

John Southworth[1], S. J. Murphy[2], K. Pavlovski[3]

[1] *Astrophysics Group, Keele University, Staffordshire, ST5 5BG, UK*

[2] *Centre for Astrophysics, University of Southern Queensland, Toowoomba, QLD 4350, Australia*

[3] *Department of Physics, Faculty of Science, University of Zagreb, Bijenicka cesta 32, 10000 Zagreb, Croatia*

ABSTRACT

We announce the discovery of pulsations in HD 23642, the only bright eclipsing system in the Pleiades, based on light curves from the Transiting Exoplanet Survey Satellite (TESS). We measure 46 pulsation frequencies and attribute them to δ Scuti pulsations in the secondary component. We find four $\ell = 1$ doublets, three of which have frequency splittings consistent with the rotation rate of the star. The dipole mode amplitude ratios are consistent with a high stellar inclination angle and the stellar rotation period agrees with the orbital period. Together, these suggest that the spin axis of the secondary is aligned with the orbital axis. We also determine precise effective temperatures and a spectroscopic light ratio, and use the latter to determine the physical properties of the system alongside the TESS data and published radial velocities. We measure a distance to the system in agreement with the *Gaia* parallax, and an age of 170 ± 20 Myr based on a comparison to theoretical stellar evolutionary models.

Key words: stars: fundamental parameters — stars: binaries: eclipsing — stars: oscillations

1 INTRODUCTION

The Pleiades is one of the closest and most extensively studied star clusters, containing ∼1300 stars at a distance of 136 pc (Melis et al. 2014; Heyl et al. 2022). It is a benchmark for studying theoretical modelling (e.g. Vandenberg & Bridges 1984) the kinematics of star clusters (Lodieu et al. 2019), binarity (Torres et al. 2021), pulsations (Murphy et al. 2022), rotation (Rebull et al. 2016), and the connection between rotation, lithium depletion and stellar inflation (Somers & Pinsonneault 2015; Bouvier et al. 2018).

Eclipsing binary stars (EBs) are another crucial research area for improving our understanding of stellar evolution (Torres et al. 2010). The masses, radii and effective temperatures ($T_{\rm eff}$s) of stars can be determined to precisions approaching 0.2% (Maxted et al. 2020; Miller et al. 2020), allowing their use as checks and calibrators of theoretical models (e.g. Claret & Torres 2018; Tkachenko et al. 2020). In particular, EBs in open clusters are enticing targets for multiple scientific goals (e.g. Southworth et al. 2004a; Brogaard et al. 2011; Torres et al. 2018).

A third phenomenon well suited to extending our understanding of stellar physics is that of pulsations. δ Scuti stars pulsate in pressure modes of low radial order ($n \sim 1 \ldots 10$) that are mostly sensitive to the stellar envelope (Aerts et al. 2010; Kurtz 2022). These modes probe the stellar density, making them good indicators of age (Aerts 2015), especially when mass and/or metallicity are already constrained. Recently, the discovery that δ Scuti stars pulsate in regular patterns (Bedding et al. 2020) has allowed pulsation modes to be identified in many stars (e.g. Kerr et al. 2022; Currie et al. 2022), including five members of the Pleiades (Murphy et al. 2022), facilitating detailed asteroseismic modelling. In some cases, this confers an age precision better than 10% (Murphy et al. 2021).

HD 23642 (V1229 Tau, HII 1431) was found to be a double-lined spectroscopic binary by Pearce (1957) and Abt (1958). Its

eclipsing nature was announced independently by Miles (1999) and Torres (2003) using data from the *Hipparcos* satellite. Detailed analyses of the system using ground-based data have been presented by Griffin (1995); Torres (2003); Munari et al. (2004); Southworth et al. (2005) and Groenewegen et al. (2007). HD 23642 was observed in long cadence mode by the K2 satellite (Howell et al. 2014) in Campaign 4[1]. An analysis of these data was presented by David et al. (2016).

In this work we present the discovery of δ Scuti pulsations in this important EB and determine the physical properties of the system to high precision for the first time. We note that independent detections are presented by Chen et al. (2022) without detailed analysis, and by Bedding et al. (2023). Section 2 in the current work outlines the observations used, Sections 3 and 4 present our spectroscopic and photometric analyses, Section 5 is dedicated to the pulsation analysis, and our work is concluded in Section 6.

2 OBSERVATIONS

HD 23642 was observed using the TESS mission (Ricker et al. 2015) in three consecutive sectors (42–44) covering 76 days (2021/08/20 to 2021/11/06), at a cadence of 120 s. We downloaded the data from the Mikulski Archive for Space Telescopes (MAST) archive and extracted the simple aperture photometry (SAP) from the FITS files (Jenkins et al. 2016); the PDCSAP data are practically identical. We included only the data with a QUALITY flag of zero, totalling 44 438 points, and converted them into differential magnitude. The data errors were not used as they were much smaller than

---

[1] HD 23642 was requested as a target by nine Guest Observer proposals including GO4028 (PI Southworth) and GO4035 (PI Murphy).
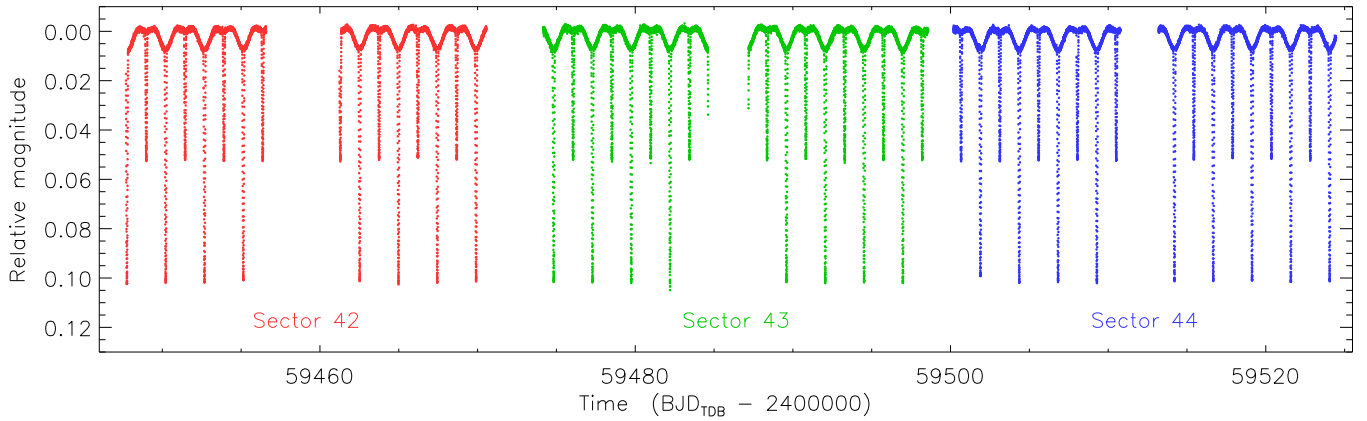
Figure 1. TESS simple aperture photometry (SAP) light curve of HD 23642. The sectors are labelled.

the scatter of the measurements. The full TESS data are shown in Fig. 1.

We observed HD 23642 during two observing runs in November 2006 using the Nordic Optical Telescope (NOT) and its FIbre Echelle Spectrograph (FIES). A total of 27 échelle spectra were obtained using the medium-resolution fibre in bundle A, which covered 364–736 nm with a resolving power of $R \approx 47\,000$. Exposure times of 600 s yielded a signal to noise ratio (S/N) of approximately 200, although some spectra had a lower S/N due to cloudy conditions. The data were reduced using IRAF échelle package routines, with particular care taken in the normalisation and merging of the échelle orders (Kolbas et al. 2015).

3 SPECTROSCOPIC ANALYSIS

We first sought to measure the spectroscopic parameters of the two stars, in particular their T_{eff}s and light ratio. To do this we applied the method of spectral disentangling (Simon & Sturm 1994) using the Fourier approach (Hadrava 1995) and concentrating on the 650-670 nm spectral range which includes the Hα line. This wavelength interval is contaminated by telluric lines, which we removed before the disentangling process. We used the FDBINARY code (Ilijić et al. 2004) and our standard methods (Pavlovski & Hensberge 2010; Pavlovski et al. 2018). We also fixed the velocity amplitudes of the stars to the values measured by Torres et al. (2021), so effectively ran in spectral separation mode.

The Hα profiles of the two stars were then modelled to determine the T_{eff}s and light ratio. We fixed the surface gravities and rotational velocities of the stars to the values determined in Section 4, thus avoiding the degeneracy between T_{eff} and $\log g$ present in the Balmer lines of hot stars. This approach required us to iterate our analysis with that described in Section 4 to ensure internal consistency; the iteration converged within one step. Optimal fitting was performed with the STARFIT code (Kolbas et al. 2015), which uses a genetic algorithm to search for the best fit within a grid of synthetic spectra pre-calculated using the UCLSYN code (Smalley et al. 2001). The fractional light contributions of the two components were forced to sum to unity (Tamajo et al. 2011) and only the wings of the Hα line were fitted (with metallic lines masked). The uncertainties were calculated using the MCMC approach described in Pavlovski et al. (2018).

We found T_{eff}s of $10\,200 \pm 90$ K and 7670 ± 85 K for the two stars, and a light ratio of $\ell_B/\ell_A(H\alpha) = 0.313 \pm 0.010$. HD 23642 A

is known to be chemically peculiar: Abt & Levato (1978) classified its spectrum as A0Vp(Si) + Am. Our light ratio should not be affected by this because it was obtained from only the Hα line. We propagated it to the TESS passband using BT-Settl theoretical spectra (Allard et al. 2012) to obtain $\ell_B/\ell_A(\mathrm{TESS}) = 0.328 \pm 0.011$ where the errorbar includes the contributions from $\ell_B/\ell_A(H\alpha)$ and both T_{eff}s.

4 LIGHT CURVE AND PHYSICAL PROPERTIES

The light curve of HD 23642 shows shallow partial eclipses and clear reflection and ellipsoidal effects. The stars are well-separated and the system is suitable for analysis with the JKTEBOP code (Southworth et al. 2004b; Southworth 2013), for which we used version 43. We fitted for the fractional radii of the stars in the form of their sum ($r_A + r_B$) and ratio ($k = r_B/r_A$), the orbital inclination (i), the central surface brightness ratio of the two stars (J), the amount of third light (L_3), the reference time of mid-eclipse (T_0), and the orbital period (P). Limb darkening was included using the power-2 law (Hestroffer 1997) with the scaling coefficient for each star (c_1 and c_2) fitted and the power-law coefficients (α_1 and α_2) fixed at values from Claret & Southworth (2022). We also included one quadratic function per TESS half-sector to normalise the light curve to zero differential magnitude, to allow for the possibility of slow drifts in brightness for either instrumental or astrophysical reasons. The pulsations are of much lower amplitude than the eclipses so were treated as red noise. A circular orbit was assumed.

Our initial solutions gave measurements of the fractional radii to a disappointing precision. This is caused by the ratio of the radii being poorly determined for shallow partial eclipses, a well-known phenomenon that has been noted before for this system (Southworth et al. 2005; David et al. 2016). We therefore imposed the spectroscopic light ratio from Section 3 as a Gaussian prior in our solution. This significantly improved the precision of the fitted parameters, and is the only viable approach in a system like this with shallow partial eclipses and a noise limit set by the presence of pulsations. Uncertainties in the fitted parameters were determined by Monte Carlo and residual-permutation simulations (Southworth 2008), taking the larger of the two options for each quantity. The values and uncertainties of the parameters are given in Table 1. We have added an extra uncertainty of ± 0.0010 in quadrature to the uncertainties in r_A and r_B to account for the variations in these param-
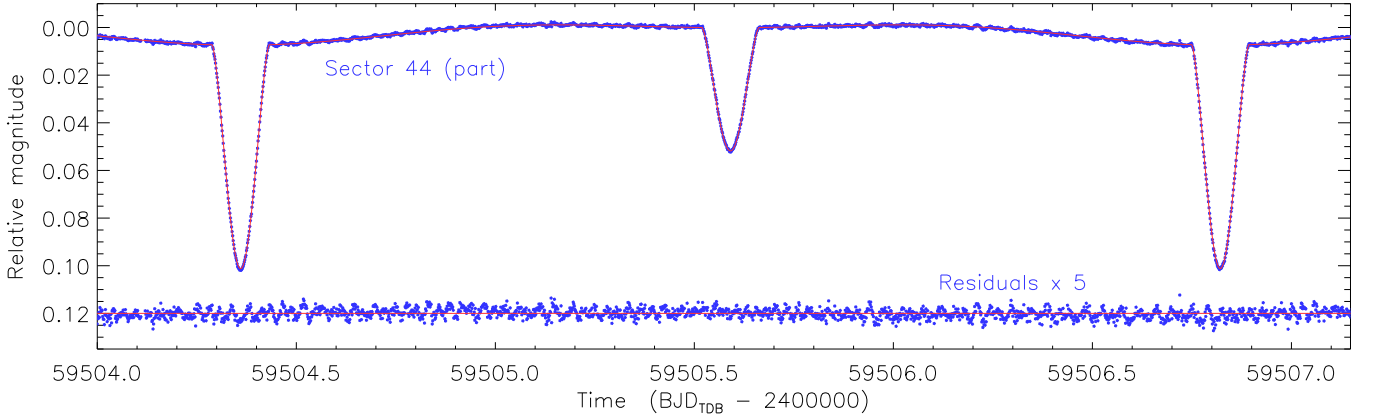
Figure 2. A short section of the TESS light curve, chosen at random, is shown (blue points) along with the JKTEBOP best fit (red line). The residuals are displayed offset to the base of the figure and magnified by a factor of 5 to make the pulsations visible.

Table 1. Properties of the HD 23642 system. The velocity amplitudes K are from Torres et al. (2021).

Quantity and unit	Star A	Star B
Spectroscopic parameters:		
K (km s^{-1})	100.07 ± 0.23	142.60 ± 0.28
$T_{\rm eff}$ (K)	10200 ± 90	7670 ± 85
Light ratio at Hα	0.313 ± 0.010	
Light ratio in TESS passband	0.328 ± 0.011	
JKTEBOP *analysis:*		
$r_{\rm A} + r_{\rm B}$	0.2664 ± 0.0011	
k	0.784 ± 0.012	
i (°)	78.63 ± 0.09	
J	0.5561 ± 0.0011	
ℓ_3	0.029 ± 0.014	
c	0.52 fixed	0.63 fixed
α	0.45 fixed	0.42 fixed
P (d)	$2.46113223 \pm 0.00000060$	
T_0 (BJD$_{\rm TDB}$)	$2459509.282357 \pm 0.000007$	
Fractional radii	0.1494 ± 0.0016	0.1171 ± 0.0017
Physical properties:		
Mass ($\mathcal{M}_\odot^{\rm N}$)	2.273 ± 0.011	1.595 ± 0.008
Radius ($\mathcal{M}_\odot^{\rm N}$)	1.799 ± 0.019	1.410 ± 0.021
$\log g$ (c.g.s.)	4.285 ± 0.009	4.342 ± 0.13
$V_{\rm synch}$ (km s^{-1})	36.98 ± 0.40	28.99 ± 0.42
Luminosity $\log(L/\mathcal{L}_\odot^{\rm N})$	1.499 ± 0.018	0.792 ± 0.023
Reddening E_{B-V} (mag)	0.040 ± 0.010	
K-band distance (pc)	134.7 ± 2.0	

eters between different model choices, specifically about whether or not to fit for L_3 or limb darkening.

We determined the physical properties of the system from the results of the JKTEBOP analysis and the velocity amplitudes of the stars measured by Torres et al. (2021). This was done using the JK-TABSDIM code (Southworth et al. 2005) modified to report results on the IAU scale (Prša et al. 2016). The full set of measured system properties are given in Table 1. Our masses are in good agreement with those found by other authors, with minor differences due to the newer velocity amplitudes adopted. The rotational velocities of the stars determined by Southworth et al. (2005), 37 ± 2 and 33 ± 3 km s^{-1}, are in agreement with the synchronous values, suggesting that both stars are rotating synchronously.

The measured radii, however, are significantly different from

previous values (Munari et al. 2004; Southworth et al. 2005; Groenewegen et al. 2007; David et al. 2016) in the sense that $R_{\rm A}$ is larger and $R_{\rm B}$ is smaller. This solves an existing problem with HD 23642 B, which was previously found to be significantly larger than predicted by theoretical evolutionary models for the Pleiades' age and metallicity. We attribute this change to differences in the spectroscopic light ratios adopted in those studies, which are slightly larger than the one measured in the current work. Both components of HD 23642 are known to be chemically peculiar so light ratios determined from metal lines are unreliable. Our new light ratio should be preferred because it is based on the Hα line so is not affected by the chemical peculiarity, and is also close to the wavelengths transmitted by the TESS passband. A visual comparison of the masses, radii and $T_{\rm eff}$s of the primary star to predictions from the PAR-SEC evolutionary models (Bressan et al. 2012) for solar metallicity shows good agreement for an age of 170 ± 20 Myr. We note that this is at the upper limit of accepted ages of the Pleiades cluster (Gossage et al. 2018; Murphy et al. 2022). The secondary component is 1.5σ smaller than expected: further investigation is needed to understand this.

To determine the distance (d) and interstellar reddening (E_{B-V}) to the system we used the BV apparent magnitudes from the Tycho satellite (Høg et al. 2000), the JHK_s apparent magnitudes from 2MASS (Skrutskie et al. 2006) converted into the Johnson system using transformations from Carpenter (2001), and bolometric corrections from Girardi et al. (2002). We determined the value of E_{B-V} that results in consistent distances across the $BVJHK$ bands, finding $E_{B-V} = 0.040 \pm 0.010$ and $d = 134.7 \pm 2.0$ pc. This distance is slightly shorter than the 138.3 ± 0.1 pc determined by simple inversion of the parallax from *Gaia* EDR3 (Gaia Collaboration 2021). This E_{B-V} is specific to HD 23642, is consistent with previous studies (Taylor 2008), and is not affected by reddening variations between Pleiades members.

5 ANALYSIS OF THE PULSATIONS

The residual light curve after subtraction of the JKTEBOP model shows several pulsation modes at the 0.1 mmag level (Fig. 3). We used the PERIOD04 code (Lenz & Breger 2004) to extract 46 pulsations at frequencies $f > 20$ d^{-1} down to 0.015 mmag amplitude, and used non-linear least squares to optimise the frequencies. The table of frequencies is given in the Appendix. From the frequencies
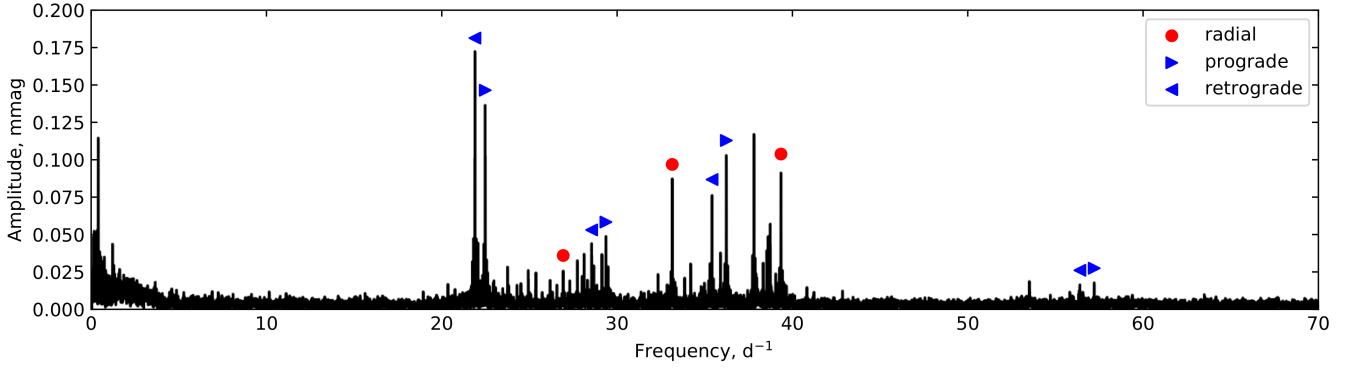
Figure 3. Fourier transform of the light curve residuals, after subtracting the eclipse model, revealing several pulsations at the 0.1 mmag level. Mode identifications (Section 5) are overlaid, showing radial modes as well as a series of rotationally split dipole modes.

and T_{eff}s of the stars we deduce that they represent δ Scuti pulsations in the secondary component, as the primary is hotter than the δ Scuti instability strip.

We used the ECHELLE package (Hey & Ball 2020) to manually find values of the asteroseismic large spacing, $\Delta\nu$, that give vertical patterns in an échelle diagram. At $\Delta\nu = 6.97\,\mathrm{d}^{-1}$, there are two parallel ridges on the left-hand side of the échelle (Fig. 4), at an x-location suggestive of $\ell = 1$ modes (Bedding et al. 2020; Murphy et al. 2021). With the same $\Delta\nu$, part of a radial mode series can also be identified, with period ratios consistent with low-order radial modes (Netzel et al. 2022). It is noteworthy that the independently-determined $\Delta\nu$ is consistent with the value of five other δ Scuti stars in the Pleiades (6.82–6.99 d^{-1}; Murphy et al. 2022), and also suggests that the system is relatively young ($\lesssim 200\,\mathrm{Myr}$).

Since $\ell = 1$ doublets are seen, which are interpretable as $m = \pm 1$ pairs, the inclination of the pulsating star is not small (Gizon & Solanki 2003). However, at some orders, most notably at $n = 3$, there is a peak slightly offset from halfway between the two identified $\ell = 1$ modes that could be a central component, after second-order effects of rotation are accounted for. To evaluate this possibility would require the calculation of rotating evolutionary and pulsation models. If confirmed, it implies that the stellar inclination is also not completely edge-on and, given the measured orbital inclination, implies that the spin and orbital axes of the pulsating star are aligned.

The identification of four $\ell = 1$ doublets offers the chance of a consistency check on the mode identification. If the doublets all have approximately the same splitting, it strengthens the proposed mode identifications. For the doublets at $n = 6, 3, 2$, and 1 we measure splittings of 0.813, 0.813, 0.812, and 0.586 d^{-1}, respectively. Thus, the $n = 6, 3$, and 2 doublets seem secure, but the $n = 1$ doublet does not. Since the Ledoux constant, $C_{n,\ell}$, is close to zero for p modes, we can estimate the stellar rotation rate, Ω, to first order based on these frequency splittings (Aerts et al. 2010):

$$\nu_{n,\ell,m} = \nu_0 + m\Omega(1 - C_{n,\ell}), \tag{1}$$

where ν_0 is the rest-frame frequency of the pulsation mode (we adopt the convention that prograde modes have positive m). The stellar rotation frequency is therefore 0.41 d^{-1}, corresponding to a rotation period of 2.46 d. This is equal to the orbital period of the system, and the stars are known to rotate approximately synchronously (see Section 4), so this supports our inference of the stellar rotational inclination.
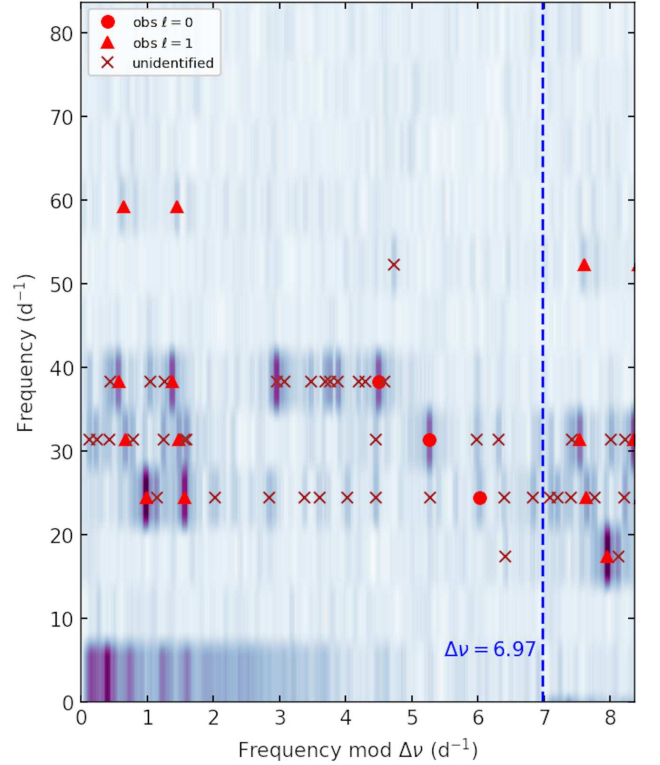
Figure 4. Échelle diagram for HD 23642, marked with mode identifications. Radial modes are shown as circles, dipole modes are triangles. Modes without an identifications are shown as crosses, some of which may belong to the other star; most will be modes of higher degree ($\ell \geq 2$).

6 SUMMARY AND CONCLUSIONS

HD 23642 has it all: youth, eclipses, pulsations, chemical peculiarity, and membership of the Pleiades. We establish its physical properties to high precision for the first time, helped particularly by the measurement of a spectroscopic light ratio immune to the chemical peculiarity. We determine a distance and interstellar reddening to the system in good agreement with previous measurements, and infer an age of $170 \pm 20\,\mathrm{Myr}$ for the Pleiades by comparison to PARSEC evolutionary model predictions.

A total of 46 pulsation frequencies are detected to high significance from the three consecutive sectors of TESS photometry. We attribute them to δ Scuti pulsations in the secondary star. We use an

échelle diagram to assign modes to 11 of the pulsations, based on the identification of $\ell = 1$ doublets. An asteroseismic large spacing of $\Delta\nu = 6.97\,\mathrm{d}^{-1}$ allows identification of a series of radial modes with period ratios consistent with other δ Scuti stars in the Pleiades. The stellar rotation rate we find from the mode splittings is in agreement with the spectroscopic $v \sin i$ and the orbital period of the system. This implies that the spin axis of the pulsating secondary component is aligned with the orbital axis of the system. HD 23642 is well suited to detailed analysis with evolutionary and pulsation models including rotation.

DATA AVAILABILITY

The TESS data used in this work are available in the MAST archive (https://mast.stsci.edu/portal/Mashup/Clients/Mast/Portal.html). The FIES spectra are available in reduced form from the NOT archive (http://www.not.iac.es/archive/).

ACKNOWLEDGEMENTS

REFERENCES

Abt H. A., 1958, ApJ, 128, 139
Abt H. A., Levato H., 1978, PASP, 90, 201
Aerts C., 2015, AN, 336, 477
Aerts C., Christensen-Dalsgaard J., Kurtz D. W., 2010, Asteroseismology. Astron. and Astroph. Library, Springer Netherlands, Amsterdam
Allard F., Homeier D., Freytag B., 2012, Philosophical Transactions of the Royal Society of London Series A, 370, 2765
Bedding T. R., et al., 2020, Nature, 581, 147
Bedding T. R., et al., 2023, AAS journals submitted, arXiv:2212.12087
Bouvier J., et al., 2018, A&A, 613, A63
Bressan A., Marigo P., Girardi L., Salasnich B., Dal Cero C., Rubele S., Nanni A., 2012, MNRAS, 427, 127
Brogaard K., Bruntt H., Grundahl F., Clausen J. V., Frandsen S., Vandenberg D. A., Bedin L. R., 2011, A&A, 525, A2
Carpenter J. M., 2001, AJ, 121, 2851
Chen X., et al., 2022, ApJS, 263, 34
Claret A., Southworth J., 2022, A&A, 664, A128
Claret A., Torres G., 2018, ApJ, 859, 100
Currie T., et al., 2022, arXiv:2212.00034
David T. J., et al., 2016, AJ, 151, 112
Gaia Collaboration 2021, A&A, 649, A1
Girardi L., Bertelli G., Bressan A., Chiosi C., Groenewegen M. A. T., Marigo P., Salasnich B., Weiss A., 2002, A&A, 391, 195
Gizon L., Solanki S. K., 2003, ApJ, 589, 1009
Gossage S., Conroy C., Dotter A., Choi J., Rosenfield P., Cargile P., Dolphin A., 2018, ApJ, 863, 67
Griffin R. F., 1995, JRASC, 89, 53
Groenewegen M. A. T., Decin L., Salaris M., De Cat P., 2007, A&A, 463, 579
Hadrava P., 1995, A&AS, 114, 393
Hestroffer D., 1997, A&A, 327, 199
Hey D., Ball W., 2020, Echelle: dynamic echelle diagrams for asteroseismology, doi:10.5281/zenodo.3629933
Heyl J., Caiazzo I., Richer H. B., 2022, ApJ, 926, 132

Høg E., et al., 2000, A&A, 355, L27
Howell S. B., et al., 2014, PASP, 126, 398
Ilijić S., Hensberge H., Pavlovski K., Freyhammer L. M., 2004, in Hilditch R. W., Hensberge H., Pavlovski K., eds, ASP Conf. Ser. Vol. 318, Spectroscopically and Spatially Resolving the Components of the Close Binary Stars. pp 111–113
Jenkins J. M., et al., 2016, in Proc. SPIE. p. 99133E
Kerr R., Kraus A. L., Murphy S. J., Krolikowski D. M., Offner S. S. R., Tofflemire B. M., Rizzuto A. C., 2022, ApJ, 941, 49
Kolbas V., et al., 2015, MNRAS, 451, 4150
Kurtz D. W., 2022, ARA&A, 60, 31
Lenz P., Breger M., 2004, in J. Zverko, J. Žižnovsky, S. J. Adelman, & W. W. Weiss ed., IAU Symposium Vol. 224, The A-Star Puzzle, Cambridge University Press, Cambridge, UK.. pp 786–790
Lodieu N., Pérez-Garrido A., Smart R. L., Silvotti R., 2019, A&A, 628, A66
Maxted P. F. L., et al., 2020, MNRAS, 498, 332
Melis C., Reid M. J., Mioduszewski A. J., Stauffer J. R., Bower G. C., 2014, Science, 345, 1029
Miles R., 1999, Journal of the British Astronomical Association, 109, 106
Miller N. J., Maxted P. F. L., Smalley B., 2020, MNRAS, 497, 2899
Munari U., Dallaporta S., Siviero A., Soubiran C., Fiorucci M., Girard P., 2004, A&A, 418, L31
Murphy S. J., Joyce M., Bedding T. R., White T. R., Kama M., 2021, MNRAS, 502, 1633
Murphy S. J., Bedding T. R., White T. R., Li Y., Hey D., Reese D., Joyce M., 2022, MNRAS, 511, 5718
Netzel H., Pietrukowicz P., Soszyński I., Wrona M., 2022, MNRAS, 510, 1748
Pavlovski K., Hensberge H., 2010, in Prša A., Zejda M., eds, Astronomical Society of the Pacific Conference Series Vol. 435, Binaries – Key to Comprehension of the Universe. p. 207
Pavlovski K., Southworth J., Tamajo E., 2018, MNRAS, 481, 3129
Pearce J. A., 1957, Publications of the Dominion Astrophysical Observatory Victoria, 10, 435
Prša A., et al., 2016, AJ, 152, 41
Rebull L. M., et al., 2016, AJ, 152, 113
Ricker G. R., et al., 2015, JATIS, 1, 014003
Simon K. P., Sturm E., 1994, A&A, 281, 286
Skrutskie M. F., et al., 2006, AJ, 131, 1163
Smalley B., Smith K. C., Dworetsky M. M., 2001, UCLSYN Userguide
Somers G., Pinsonneault M. H., 2015, MNRAS, 449, 4131
Southworth J., 2008, MNRAS, 386, 1644
Southworth J., 2013, A&A, 557, A119
Southworth J., Maxted P. F. L., Smalley B., 2004a, MNRAS, 349, 547
Southworth J., Maxted P. F. L., Smalley B., 2004b, MNRAS, 351, 1277
Southworth J., Maxted P. F. L., Smalley B., 2005, A&A, 429, 645
Tamajo E., Pavlovski K., Southworth J., 2011, A&A, 526, A76
Taylor B. J., 2008, AJ, 136, 1388
Tkachenko A., et al., 2020, A&A, 637, A60
Torres G., 2003, Informational Bulletin on Variable Stars, 5402
Torres G., Andersen J., Giménez A., 2010, A&ARv, 18, 67
Torres G., Curtis J. L., Vanderburg A., Kraus A. L., Rizzuto A., 2018, ApJ, 866, 67
Torres G., Latham D. W., Quinn S. N., 2021, ApJ, 921, 117
Vandenberg D. A., Bridges T. J., 1984, ApJ, 278, 679

APPENDIX A: MEASURED PULSATION FREQUENCIES IN HD 23642

This paper has been typeset from a TEX/LATEX file prepared by the author.

Table A1. Extracted frequencies with corresponding amplitudes and provisional mode identifications for the pulsating component of HD 23642.

f (d^{-1})	amplitude (mmag)	n	ℓ	m
57.2112	0.0175	6	1	1
56.3981	0.0161	6	1	−1
36.2304	0.1029	3	1	1
35.4177	0.0768	3	1	−1
29.3618	0.0483	2	1	1
28.5496	0.0431	2	1	−1
22.4772	0.1365	1	1	1
21.8913	0.1713	1	1	−1
39.3467	0.0938	4	0	0
33.1444	0.0869	3	0	0
26.9261	0.0260	2	0	0
53.5132	0.0188	–	–	–
39.4291	0.0302	–	–	–
39.1434	0.0157	–	–	–
39.0450	0.0199	–	–	–
38.7352	0.0514	–	–	–
38.6162	0.0407	–	–	–
38.5353	0.0362	–	–	–
38.3290	0.0296	–	–	–
37.9217	0.0272	–	–	–
37.8036	0.1171	–	–	–
36.1084	0.0165	–	–	–
35.8956	0.0370	–	–	–
35.2961	0.0289	–	–	–
34.1939	0.0286	–	–	–
33.8544	0.0206	–	–	–
32.3307	0.0221	–	–	–
29.4768	0.0239	–	–	–
29.4484	0.0198	–	–	–
29.1269	0.0368	–	–	–
28.6681	0.0302	–	–	–
28.3104	0.0203	–	–	–
28.1144	0.0378	–	–	–
28.0038	0.0230	–	–	–
27.7391	0.0347	–	–	–
27.3022	0.0181	–	–	–
26.1835	0.0203	–	–	–
25.3700	0.0252	–	–	–
24.9365	0.0264	–	–	–
24.5100	0.0159	–	–	–
24.2900	0.0160	–	–	–
23.7500	0.0281	–	–	–
22.9355	0.0181	–	–	–
22.0604	0.0403	–	–	–
20.3501	0.0157	–	–	–